Published in final edited form as:
Kidney Int. 2012 January ; 81(2): 152–159. doi:10.1038/ki.2011.332.

Detection of glomerular complement C3 fragments by magnetic resonance imaging in murine lupus nephritis

S. Anna Sargsyan, Ph.D.[1,*], **Natalie J. Serkova, Ph.D.**[2], **Brandon Renner, M.S.**[1], **Kendra M. Hasebroock, B.S.**[2], **Brian Larsen, Ph.D.**[3], **Conrad Stoldt, Ph.D.**[3], **Matthew C. Pickering, M.D.**[4], **Kim McFann, Ph.D.**[1], and **Joshua M. Thurman, M.D.**[1]

[1]Department of Medicine, University of Colorado Denver School of Medicine, Aurora, CO, 80045, USA

[2]Department of Anesthesiology, University of Colorado Denver School of Medicine, Aurora, CO, 80045, USA

[3]Department of Mechanical Engineering, University of Colorado Boulder, UCB 427, Boulder, CO, 80309, USA

[4]Molecular Genetics and Rheumatology Section, Faculty of Medicine, Imperial College, Hammersmith Campus, London, UK

Abstract

One of the challenges of treating patients with glomerulonephritis (GN) is to accurately assess disease activity. We recently developed a magnetic resonance imaging (MRI)-based method of detecting glomerular C3, and hypothesized that this agent could be used to monitor the severity of GN. In the current study we used this imaging method to track the progression of renal disease in the MRL/lpr mouse model of lupus nephritis (LN). The targeting agent is comprised of superparamagnetic iron oxide (SPIO) nanoparticles conjugated to complement receptor type 2 (CR2-targeted SPIO). Glomerular C3b/iC3b/C3d deposition in progressively aging MRL/lpr and control mice was monitored with quantitative immunofluorescence or with CR2-targeted SPIO and T2-weighted MRI. Immunofluorescence showed that glomerular C3b/iC3b increased with disease activity. This finding was replicated with the T2-weighted MRI: T2-relaxation times decreased (as SPIO reduce T2-relaxation times) with disease activity in the cortex and medullas of MRL/lpr mice, but not of control mice. Our findings demonstrate that an MRI contrast agent targeted to glomerular C3b/iC3b/C3d can be used to non-invasively monitor disease activity in GN. Further, therapeutic complement-inhibitors have recently been used in patients with renal disease, and this method could identify patients likely to benefit from complement inhibition.

Keywords

CR2-targeted iron oxide nanoparticles; T2-relaxation time; glomerulonephritis

[*]Corresponding author: Siranush Anna Sargsyan, Division of Renal Diseases and Hypertension, Department of Medicine, University of Colorado Denver School of Medicine, Campus Box B115, University of Colorado Denver, Aurora, CO, 80045, office phone: 303-724-2494, fax: 303-724-7581, siranush.sargsyan@ucdenver.edu.
Current address for BL is National Renewable Energy Laboratory, Golden, CO.

DISCLOSURES
JMT is a consultant for Alexion Pharmaceuticals, Inc.

INTRODUCTION

New biomarkers for the detection and surveillance of glomerulonephritis would be of immense clinical utility.[1] The current standard for diagnosing glomerulonephritis is a percutaneous renal biopsy. This procedure provides much useful information about the etiology and activity of the underlying disease. Biopsies sample only a small proportion of the kidney, however, and complications occur in approximately 6 percent of patients.[2–4] Less invasive methods of obtaining the information yielded by biopsies would be of great clinical benefit.

The involvement of complement cascade proteins in renal diseases is well documented. Whether circulating, or locally produced, complement cascade proteins and their proteolytically generated fragments (i.e., fragments of C3 and C4) are deposited on the glomerulocapillary, mesangial and tubulointerstitial cells during many types of renal injury.[5] Notably, C3 and C4 fragments are covalently attached to these sites. Renal biopsies are routinely stained for deposits of C3 activation fragments (C3b/iC3b/C3d), and glomerular C3 deposits are found in most forms of glomerulonephritis.[6] Biopsy series of patients with lupus nephritis have correlated the presence of C3 fragments with the morphologic classification, although the extent of glomerular C3 fragment deposition was not rigorously quantified.[7]

Superparamagnetic iron oxide (SPIO, 60–150 nm in diameter) particles and ultrasmall superparamagnetic iron oxide (USPIO, 5–40 nm in diameter) particles can be used as T2-based negative contrast agents for magnetic resonance imaging (MRI).[8] Furthermore, by conjugating SPIO to vectors that bind specific molecules, the SPIO can be used to detect those molecular targets *in vivo*. Using this approach, we have previously developed targeted SPIO and a T2-mapping MRI protocol to detect intra-renal C3b/iC3b/C3d deposits in the kidneys of 16 weeks old MRL/lpr mice.[9] The targeted SPIO were developed through conjugation with a chimeric molecule CR2-Fc, generating CR2-targeted SPIO. The molecule is comprised of the first two short consensus repeats of human complement receptor type 2 (CR2) that has a specificity to iC3b/C3d complement fragments,[10] and mouse Ig constant region (Fc).

In the current study we sought to determine whether the abundance of C3b/iC3b/C3d deposition in the kidney can serve as a good biomarker of disease onset and severity, and whether their deposition in the kidneys can be monitored non-invasively using CR2-targeted SPIO and T2-weighted MRI. To accomplish this, we examined cohorts of MRL/lpr mice and MRL/Mpj control mice as they aged. We used quantitative immunofluorescence to correlate C3b/iC3b/C3d abundance in the glomerular and tubular compartments of the kidney with the age of the mice. We then tracked the kidney C3b/iC3b/C3d deposition by T2-weighted MRI: cohorts of MRL/lpr and control mice, at various ages, were injected with CR2-targeted SPIO and T2-relaxation times were calculated from MRI scans. Reduction in T2-relaxation times, induced by CR2-targeted SPIO, was correlated with the age of the mice to determine whether it would reflect C3b/iC3b/C3d deposition in the kidneys.

MATERIALS AND METHODS

Animals

MRL/lpr and MRL/Mpj mice were purchased from the Jackson Laboratory. The animals were housed under standard laboratory conditions (a 12 hour (h) light/dark cycle, standard food and water ad libitum). In the present study, two cohorts of mice were used: one cohort, consisting of 7 MRL/lpr and 4 MRL/Mpj mice, was followed from ages 12 to 24 weeks with monthly injections of CR2-targeted SPIO and MRI scans. Another cohort, consisting of 9

MRL/lpr mice, was used for histological analysis. Three mice each were sacrificed at 8, 16 and 22 weeks of age. Tissues and serum were obtained for analysis. Although we had planned on harvesting the oldest group of mice at 24 weeks of age to match the MRI cohort, the mice appeared ill and were sacrificed early for humane reasons. To confirm that deposition of the CR2-targeted SPIO in the glomeruli was mediated by the interaction of CR2 with glomerular C3d, we have also utilitized mice with targeted deletion of the factor H gene ($fH^{-/-}$ mice) (*FN*). These mice have abuandant glomerular C3d, but do not have detectable glomerular IgG deposits. All animal procedures were approved by the University of Colorado Denver animal care and use committee. The animal care before and during the experimental procedures was conducted in accordance with the policies of National Institute of Health Guide for the Care and Use of Laboratory Animals.

Immunostaining

To assess whether the abundance of glomerular C3 fragment deposits increases in age-dependent manner, the kidneys of MRL/lpr mice at 8, 16 and 22 weeks were examined by immunofluorescence microscopy for C3b/iC3b and C3d. The kidneys were harvested, snap-frozen, and stored at −80 °C until used. Seven μm-thick kidney sections of MRL/lpr mice were fixed with acetone for 1 minute (min), and then rehydrated with phosphate-buffered saline (PBS). The sections were blocked in 10 percent normal goat serum (Jackson ImmunoResearch) for 1 h at room temperature, then incubated with primary antibodies [polyclonal goat anti-C3-fluorescein isothiocyanate (FITC)-conjugated antibody (Cappel) that does not recognize C3d fragment by Western blot, polyclonal rabbit anti-human C3d (Dako, this antibody may also recognize C3dg), rat anti-mouse F4/80 (Caltag) and rat anti-mouse CD11b-phycoerythrin (PE)-conjugated antibody (Caltag)] for 1 h, at room temperature. After 5 washes with PBS, 5 min each, the sections were mounted directly in VectaShield (Vector Laboratories), or incubated with secondary antibodies [anti-rabbit-IgG-FITC (Jackson ImmunoResearch, and anti-rat-IgG-Alexa-594 (Invitrogen)] for 1 h at room temperature, washed again, and then mounted. The images were acquired under 40x and 10x objectives with an Olympus BX51 microscope and a digital camera (Pixera). To quantify relative fluorescence units (RFU), regions of interest (ROI) were drawn around glomeruli, or tubules, and mean fluorescence values obtained with the “Measure” plugin of ImageJ software. RFU were measured from 10 glomeruli, or 10 tubules from each kidney compartment, per mouse per age.

Synthesis of SPIO, conjugation with CR2-Fc and test for C3 binding

The SPIO were synthesized and functionalized for conjugation to proteins as described previously.[11, 12] The SPIO were conjugated with CR2-Fc as described previously.[9] The presence of CR2-Fc on the surface of conjugated SPIO was confirmed using fluorescence activated cell sorting (FACS) analysis with a biotinylated anti-CR2 antibody 171[13] and streptavidin-PE (SA-PE). The functionality of the bound CR2-Fc molecules on the surface of CR2-targeted SPIO was confirmed in a binding assay with opsonized Chinese hamster ovary (CHO) cells. First, the CHO cells at 10^6 cells/tube were incubated 200 μl of 10 percent normal mouse serum in PBS at 37 °C to induce opsonization with C3 fragments. The presence of C3 fragments on the surface of CHO cells was checked with FACS analysis and a directly labeled goat polyclonal anti-C3-FITC antibody (Cappel). The opsonized CHO cells, at 10^6 cells/tube, were incubated with 20 μl of CR2-targeted SPIO. The antibody 171, used biotinylated or unmanipulated, was added to cell/SPIO mixture. After 1h incubation, SA-PE was added to all tubes, and following another 1 h incubation, the cell/SPIO/antibody/SA-PE mixture was washed with PBS, and examined by FACS analysis. All flow cytometry analyses were conducted with FACSCalibur (BD Biosciences) and CellQuest Pro software.

T2-Weighted MRI mapping for calculations of T2-relaxation times

12 weeks old MRL/lpr mice (lupus group, n = 7) and MRL/Mpj control animals (n = 4) were assessed by T2-weighted MRI at baseline and 48 h after CR2-targeted SPIO injection (0.4 mg, or 10–16 mg/kg). The MRI scans were repeated serially at 16, 20, and 24 weeks of age. As expected from the incidence of mortality of 40 percent for the 16 weeks old and 80 percent for the 24 weeks old MRL/lpr mice,[14] only two mice (out of seven) reached the age of 24 weeks. The mortality was unlikely to have been caused or accelerated with the injection of CR2-targeted SPIO, as the incidence of mortality matched that reported in literature, and all 4 mice in the control MRL/Mpj cohort completed the study.

Anesthetized animals were inserted into a 4.7 Tesla Bruker PharmaScan MRI scanner. A Bruker volume coil (32 mm diameter), tuned to the ^{1}H frequency of 200 MHz, was used for radiofrequency (RF) transmission and reception. A series of multi slice multi echo (MSME) T2-weighted pulses with 16 various echo times was applied for precise T2 mapping and calculation of T2-relaxation times. The scan parameters were as follows: field of view (FOV)=4.00 cm; slice thickness 1.50 mm; inter-slice distance 1.80 mm; repetition time TR=2,650 ms; time to echo (TE)1=10 ms; TE2=20 ms (followed by 30, 40, 50, 60, 70, 80, 90, 100, 110, 120, 130, 140, 150, 160 ms); slice orientation axial; number of slices 16; number of averages 2; matrix size 128x256; total acquisition time 11 min. The T2-relaxation times (in milliseconds, ms) of kidney cortex, inner and outer medulla, as well as muscle (as a control tissue), were calculated with Bruker ParaVision software. The Bruker t2vtr-fitting function, based on the equations below, was applied to calculate T2 times:

1. $S = M_0(1- e^{-TR/T1})e^{-TE/T2}$
2. $S = C_2e^{-TE/T2}$

where S is signal intensity, M_0 is magnetization, TR is time to repeat, T1 is spin-lattice relaxation time, TE is time to echo, T2 is spin-spin relaxation time, and C_2 is a constant (= $M_0(1- e^{-TR/T1})$). A visual representation of the changes in S with increasing TE is presented in Supplementary Figure S1. Delta T2-relaxation times (ΔT2-relaxation times) were calculated by subtracting the higher T2-relaxation time values at the baseline from the lower T2-relaxation time values at 48 h after SPIO injection for the same tissue of the same animal. This resulted in negative ΔT2-relaxation time values as the bound SPIO reduced/shortened the T2-relaxation time.

Statistical analyses

Unless indicated otherwise, the data are reported as mean ± standard error of the mean (SEM). Correlation of non-longitudinal data of RFU with age (histological assessment of kidneys from 9 MRL/lpr mice at ages 8, 16 and 22 weeks), all of which were single time-point measurements for each mouse at each age, was evaluated using linear regression analysis with Prism 5.0 software. Where there were repeated measures on the same mice (the longitudinal MRI study with 7 MRL/lpr and 4 MRL/Mpj mice and monthly injections of CR2-targeted SPIO at 12, 16, 20 and 24 weeks of age), mixed model longitudinal data analysis with pre-planned contrasts was used (to analyze the ΔT2-relaxation times between MRL/lpr and MRL/Mpj (control) mice, and the effect of mouse age on ΔT2-relaxation times) with SAS 9.2 statistical software. P value of less than 0.05 was considered significant.

RESULTS

In MRL/lpr mice, progression of kidney dysfunction is age-dependent. Proteinuria is absent at 8 weeks of age, but its incidence increases to 40 percent by 16 weeks, and to 80 percent by 24 weeks. The MRL/lpr strain exhibits 80 percent mortality from renal dysfunction at 24

weeks of age.[14] While the MRL/lpr model is well characterized, none of the studies, to our knowledge, document age-dependent glomerular changes in C3 fragment deposition, and whether glomerular C3b/iC3b/C3d can be used as biomarkers of disease activity. To address this gap, the kidneys of MRL/lpr mice were studied for C3 fragment deposition (Figure 1a) at different ages reflective of age-dependent kidney dysfunction.[14] The kidneys of 8, 16 and 22 week-old MRL/lpr mice were immunostained for C3b and iC3b (collectively referred to as C3b/iC3b hereafter) with a polyclonal anti-C3 antibody, and for C3d with a polyclonal anti-C3d antibody. Glomerular C3b/iC3b deposition was detected at 8 weeks, but progressively increased up to 22 weeks of age, and positively correlated with age in the MRL/lpr mice (Figure 1b and c). Glomerular C3d deposition was also detected at 8 weeks, increased at 16 weeks of age, but showed a small decrease at 22 weeks (Figure 1b and d). Additionally, the glomeruli of MRL/lpr mouse kidneys displayed hypercellularity, periglomerular infiltrates of monocytes/macrophages, increased glomerular surface area, and decreased renal function by 22 weeks of age (Supplementary Figures S2 and S3).

Next, we examined the deposition of C3b/iC3b and C3d in the renal tubulointerstitium of MRL/lpr mice. The staining pattern for C3b/iC3b/C3d on the tubules of MRL/lpr kidneys displayed minimal changes with age (Figure 2). A trend towards reduced C3b/iC3b/C3d deposition with increasing age was noted on tubules of MRL/lpr kidney cortex, outer and inner medullae (Figure 2a and b). At 22 weeks, the C3b/iC3b levels on the tubules of inner medulla of MRL/lpr mice showed a small increase relative to the C3b/iC3b levels at 16 weeks, but the RFU remained low. Overall, these findings demonstrate that disease progression in MRL/lpr mice is characterized by increasing C3b/iC3b/C3d deposition in the glomeruli, but largely unchanged C3b/iC3b/C3d deposition in the tubulointerstitium.

In order to non-invasively track the deposition of C3b/iC3b/C3d in the kidneys of MRL/lpr mice, we generated a T2-weighted MRI contrast agent – CR2-targeted SPIO (as described in Materials and Methods section). The CR2-targeted SPIO were tested for binding to C3 fragments *in vitro* (Figure 3) and *in vivo* (Supplemental Figure 4). The CR2-targeted SPIO were detected in glomeruli of MRL/lpr mice and did not co-localize with macrophages (Supplemental Figure 5).

To non-invasively monitor complement C3b/iC3b/C3d deposition in the MRL/lpr kidneys, the same cohorts of MRL/lpr (n = 7) and MRL/Mpj (control, n = 4) mice were injected with CR2-targeted SPIO at 12, 16, 20 and 24 weeks of age. MRI images of the kidneys were obtained prior to and 48 h after each SPIO injection. Figure 4 illustrates representative T2-weighted MR images from 12 and 24 weeks old MRL/lpr and MRL/Mpj mice obtained before and 48 h following SPIO injection. T2-relaxation times (a quantitative output of T2-weigted MRI signal) were determined for kidney cortices, outer medullae, inner medullae, and for muscle. The method of T2-relaxation time calculation is detailed in the Methods section.

A change in T2-relaxation times from pre- to 48 h post-SPIO injection value (ΔT2-relaxation time) was calculated for muscle and for left and right kidneys. To establish if MRL/lpr and MRL/Mpj kidneys differed following CR2-targeted SPIO injection, the ΔT2-relaxation times for MRL/lpr and MRL/Mpj kidneys and muscle were plotted against the age of the mice. The results are presented in Figure 5. Muscle was used as a control tissue, and the ΔT2-relaxation times of the muscles of MRL/Mpj or MRL/lpr mice were similar (Figure 5a and Supplementary Table S1). The kidney cortex, outer and inner medullae of MRL/lpr mice showed significant reductions in ΔT2-relaxation times at 12, 16 and 20 weeks of age when compared to those of MRL/Mpj mice (Figure 5b–d for left kidney only, the right kidney showed similar differences, Supplementary Table S1).

(*insert description of results for new experiments. Give callouts to supplemental figures. Can comment here on appearance of iron staining and results using anti IgG in fH mice. *).

To examine if the progression of disease in MRL/lpr mice can be monitored non-invasively using MRI, the calculated ΔT2-relaxation times for the tissues of MRL/lpr mice at different ages were compared to each other. The data are presented in Figure 5 and Supplementary Table S2. While there was no change in the muscle ΔT2-relaxation times with age, a significant reduction in ΔT2-relaxation times was observed for cortex, outer and inner medullae of MRL/lpr kidneys at 20 weeks when compared to earlier ages. This observation is consistent with the increase in C3b/iC3b deposition with age in the kidneys of MRL/lpr mice. In MRL/Mpj mice, ΔT2-relaxation times generally did not change with age.

DISCUSSION

The present study was conducted to test two hypotheses: 1) whether the abundance of glomerular C3b/iC3b/C3d deposition can serve as a marker of glomerulonephritis disease progression, and 2) whether CR2-targeted SPIO, directed to deposited C3 fragments, can track C3b/iC3b/C3d deposition by quantitative T2-weighted MRI. We demonstrated that as the MRL/lpr mice age, their kidneys exhibited an increase in glomerular C3b/iC3b/C3d deposition. At the latest time-point examined, at 22 weeks of age, the glomerular C3d deposition decreased slightly relative to that at 16 weeks. Also, CR2-targeted SPIO reduced T2-relaxation times in the cortex of MRL/lpr mouse kidneys, but not in that of control mouse kidneys. This reduction was age-dependent (except for the last time-point when glomerular C3d also decreased). Overall, the reduction in the T2 relaxation time corresponded with C3d deposition in the kidney cortex, indicating that the CR2-targeted SPIO may be useful for non-invasive monitoring of complement fragment deposition within the kidney. Thus, our findings demonstrate that glomerular C3b/iC3b/C3d deposition is a marker of glomerulonephritis activity and its accumulation in the kidneys can be non-invasively and repeatedly monitored with CR2-targeted SPIO and MRI.

Our study also revealed that the relative amounts of C3b/iC3b and C3d deposition in the glomeruli of aging MRL/lpr mice diverged at the last time-point. The conversion of bound C3, or more precisely of C3b, to iC3b and then further to C3d, on human kidney podocytes is mediated by complement receptor 1 (CR1) and factor I. The expression of CR1 is reduced in human nephritic kidneys[16] but the expression of its mouse homolog in MRL/lpr kidneys has not been studied. It is possible that the expression of the CR1 homologue in the MRL/lpr mice follows the same reduced pattern as that in humans, which would explain the decreased C3d deposition seen in the glomeruli of 22 week-old MRL/lpr kidneys.

The magnitude of negative enhancement by CR2-targeted SPIO seemed to decrease between 20 and 24 weeks. This may be due to the decrease in conversion of iC3b to C3d in the older mice. Unfortunately only a small number of mice survived to this age in our study, so our analysis of this time-point is less accurate than for the preceding time-points. An unexplained finding of this study was that the CR2-targeted SPIO reduced T2-relaxation times in the inner medullae of MRL/lpr kidneys in spite of the fact that there is little C3b/iC3b/C3d at this location. This signal reduction requires CR2 targeting[9] and it is not seen in control mice. It is possible, therefore, that during intra-renal trafficking of CR2-targeted SPIO, the CR2 interaction “traps” them within the diseased kidney. The main route of clearance of SPIO is the reticuloendothelial system (liver, spleen, lymph nodes and bone marrow).[17–19] Since CR2-targeted SPIO accumulate in the kidneys of MRL/lpr mice, it is possible that the particles are phagocytosed and metabolized by local dendritic cells and macrophages. The surface CR2-Fc protein of the retained particles may also mediate subsequent uptake via Fc receptors on nearby macrophages. Finally, it is also possible that

as the retained CR2-targeted SPIO break down within the kidneys, iron-containing products are metabolized by the tubular epithelial cells. Thus, our non-invasive method for tracking disease activity in lupus nephritis will benefit from optimization of the SPIO vectorization in order to achieve precise tissue targeting and greater MRI contrast.

Nonetheless, this technique can be a useful adjunct to current methods for monitoring glomerulonephritis, such as percutaneous renal biopsies. This non-invasive method of detecting C3 fragments in the kidneys can report not only on inflammatory activity in the kidneys, but also on the organ size and contour. Moreover, this method permits the evaluation of both kidneys in their entirety, thus it may be less susceptible to sample error than renal biopsies. Because of the non-invasive nature of this method, obtaining serial data for an individual patient may be more feasible than with repeated renal biopsies. The method, therefore, can be used to estimate the activity of the underlying disease or monitor the response of a patient to therapy. Therapeutic complement inhibitors have entered clinical use for patients with renal disease.[20] Monitoring the state of intra-renal complement activation may be particularly useful in patients who are candidates for complement inhibitory therapy. Finally, CR2-targeted SPIO can also be used to detect deposition of C3 fragments in other tissues.

Untargeted SPIO and USPIO have been used to detect renal inflammation in numerous animal studies.[21–27] More recently they have been used in several human studies, including a study to detect macrophage infiltration in glomerulonephritis and renal allograft rejection in humans.[28] In addition, untargeted iron oxide-based contrast agents have been recently introduced into clinical practice after their FDA approval; they possess no known toxic side-effects. This evidence suggests that iron-oxide-based contrast agents are safe, even in patients with kidney disease.[29]

In conclusion, we have found that glomerular C3b/iC3b/C3d deposition is a marker of glomerulonephritis in MRL/lpr mice and its accumulation in the kidneys can be non-invasively and repeatedly monitored with CR2-targeted SPIO and T2-weighted MRI. This method may be applicable to monitoring progression of lupus nephritis, or its response to therapies, with several advantages over currently available biomarkers: this method is non-invasive, it can be applied longitudinally without the need for repeat renal biopsies, and it reports on complement activation throughout both kidneys. Overall, this method may improve our ability to monitor disease activity, disease progression, and the response to therapy.

Supplementary Material

Refer to Web version on PubMed Central for supplementary material.

Acknowledgments

This work was supported by funding from the Schweppe Foundation, from the Lupus Research Institute (JMT), the University of Colorado Cancer Center Core grant (NCI P30 CA046934-14), and the Colorado Clinical and Translational Science Award (CTSA UL1 RR025780).

References

1. Meyers C, Geanacopoulos M, Holzman L, et al. Glomerular disease workshop. J Am Soc Nephrol. 2005; 16:3472–3476. [PubMed: 16267152]
2. Eiro M, Katoh T, Watanabe T. Risk factors for bleeding complications in percutaneous renal biopsy. Clin Exp Nephrol. 2005; 9:40–45. [PubMed: 15830272]

3. Stiles K, Yuan C, Chung E, et al. Renal biopsy in high-risk patients with medical diseases of the kidney. Am J Kidney Dis. 2000; 36:419–433. [PubMed: 10922324]
4. Whittier W, Korbet S. Renal biopsy: update. Curr Opin Nephrol Hypertens. 2004; 13:661–665. [PubMed: 15483458]
5. Sacks S, Zhou W. New boundaries for complement in renal disease. J Am Soc Nephrol. 2008; 19:1865–1869. [PubMed: 18256351]
6. Verroust P, Wilson C, Cooper N, et al. Glomerular complement components in human glomerulonephritis. J Clin Invest. 1974; 53:77–84. [PubMed: 4586873]
7. Hill G, Hinglais N, Tron F, et al. Systemic lupus erythematosus. Morphologic correlations with immunologic and clinical data at the time of biopsy. Am J Med. 1978; 64:61–79. [PubMed: 341703]
8. Laurent S, Forge D, Port M, et al. Magnetic iron oxide nanoparticles: synthesis, stabilization, vectorization, physicochemical characterizations, and biological applications. Chem Rev. 2008; 108:2064–2110. [PubMed: 18543879]
9. Serkova N, Renner B, Larsen B, et al. Renal inflammation: targeted iron oxide nanoparticles for molecular MR imaging in mice. Radiology. 2010; 255:517–526. [PubMed: 20332377]
10. Gilbert H, Asokan R, Holers V, et al. The 15 SCR flexible extracellular domains of human complement receptor type 2 can mediate multiple ligand and antigen interactions. J Mol Biol. 2006; 362:1132–1147. [PubMed: 16950392]
11. Barker A, Cage B, Russek S, et al. Ripening during magnetite nanoparticle synthesis: resulting interfacial defects and magnetic properties. Journal of Applied Physics. 2005; 98:063528.
12. Larsen B, Haag M, Serkova N, et al. Controlled aggregation of superparamagnetic iron oxide nanoparticles for the development of molecular magnetic resonance imaging probes. Nanotechnology. 2008; 19:265102. [PubMed: 21828671]
13. Guthridge JM, Young K, Gipson MG, et al. Epitope mapping using the X-ray crystallographic structure of complement receptor type 2 (CR2)/CD21: identification of a highly inhibitory monoclonal antibody that directly recognizes the CR2-C3d interface. J Immunol. 2001; 167:5758–5766. [PubMed: 11698449]
14. Haas C, Ryffel B, Le Hir M. IFN-gamma is essential for the development of autoimmune glomerulonephritis in MRL/Ipr mice. J Immunol. 1997; 158:5484–5491. [PubMed: 9164971]
15. Bao L, Zhou J, Holers V, et al. Excessive matrix accumulation in the kidneys of MRL/lpr lupus mice is dependent on complement activation. J Am Soc Nephrol. 2003; 14:2516–2525. [PubMed: 14514729]
16. Moll S, Miot S, Sadallah S, et al. No complement receptor 1 stumps on podocytes in human glomerulopathies. Kidney Int. 2001; 59:160–168. [PubMed: 11135068]
17. Brigger I, Dubernet C, Couvreur P. Nanoparticles in cancer therapy and diagnosis. Adv Drug Deliv Rev. 2002; 54:631–651. [PubMed: 12204596]
18. Choi H, Liu W, Liu F, et al. Design considerations for tumour-targeted nanoparticles. Nat Nanotechnol. 2010; 5:42–47. [PubMed: 19893516]
19. Peer D, Karp J, Hong S, et al. Nanocarriers as an emerging platform for cancer therapy. Nat Nanotechnol. 2007; 2:751–760. [PubMed: 18654426]
20. Davin J, Gracchi V, Bouts A, et al. Maintenance of kidney function following treatment with eculizumab and discontinuation of plasma exchange after a third kidney transplant for atypical hemolytic uremic syndrome associated with a CFH mutation. Am J Kidney Dis. 2010; 55:708–711. [PubMed: 19854549]
21. Beckmann N, Cannet C, Fringeli-Tanner M, et al. Macrophage labeling by SPIO as an early marker of allograft chronic rejection in a rat model of kidney transplantation. Magn Reson Med. 2003; 49:459–467. [PubMed: 12594748]
22. Hauger O, Delalande C, Deminière C, et al. Nephrotoxic nephritis and obstructive nephropathy: evaluation with MR imaging enhanced with ultrasmall superparamagnetic iron oxide-preliminary findings in a rat model. Radiology. 2000; 217:819–826. [PubMed: 11110949]
23. Jo S, Hu X, Kobayashi H, et al. Detection of inflammation following renal ischemia by magnetic resonance imaging. Kidney Int. 2003; 64:43–51. [PubMed: 12787394]

24. Laissy J, Idée J, Loshkajian A, et al. Reversibility of experimental acute renal failure in rats: assessment with USPIO-enhanced MR imaging. J Magn Reson Imaging. 2000; 12:278–288. [PubMed: 10931591]

25. Trillaud H, Degrèze P, Combe C, et al. USPIO-enhanced MR imaging of glycerol-induced acute renal failure in the rabbit. Magn Reson Imaging. 1995; 13:233–240. [PubMed: 7739365]

26. Yang D, Ye Q, Williams M, et al. USPIO-enhanced dynamic MRI: evaluation of normal and transplanted rat kidneys. Magn Reson Med. 2001; 46:1152–1163. [PubMed: 11746582]

27. Ye Q, Yang D, Williams M, et al. In vivo detection of acute rat renal allograft rejection by MRI with USPIO particles. Kidney Int. 2002; 61:1124–1135. [PubMed: 11849467]

28. Hauger O, Grenier N, Deminère C, et al. USPIO-enhanced MR imaging of macrophage infiltration in native and transplanted kidneys: initial results in humans. Eur Radiol. 2007; 17:2898–2907. [PubMed: 17929025]

29. Neuwelt E, Hamilton B, Varallyay C, et al. Ultrasmall superparamagnetic iron oxides (USPIOs): a future alternative magnetic resonance (MR) contrast agent for patients at risk for nephrogenic systemic fibrosis (NSF)? Kidney Int. 2009; 75:465–474. [PubMed: 18843256]

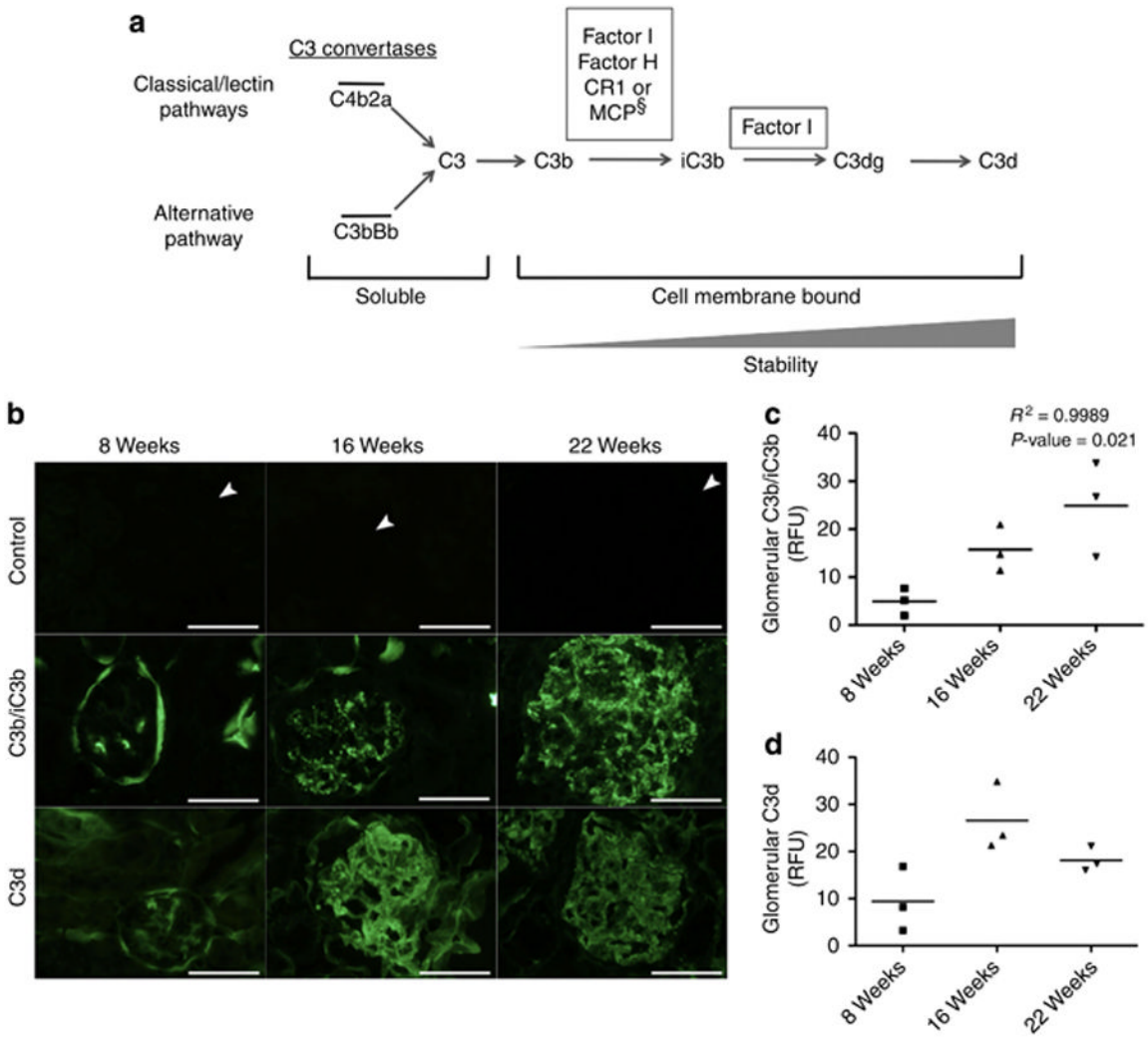

Figure 1. Glomerular C3b/iC3b/C3d deposition in MRL/lpr mice increases as the mice age

(**a**) Schematic diagram of conversion of soluble C3 to C3 fragments. § Regulators of complement activation: CR1 – complement receptor type 1; MCP – membrane co-factor protein. (**b**) Immunostaining of MRL/lpr kidneys for C3b/iC3b (middle panel) and C3d (bottom panel). No staining is seen when the anti-C3-FITC antibody is omitted (top panel, arrowheads point to glomeruli). (**c**) Quantification of relative fluorescence units (RFU) shows an increase in C3b/iC3b deposition in glomeruli of MRL/lpr kidneys with disease progression (from ages 8, 16 and 22 weeks; n = 3 mice per age group; RFU for each mouse is a mean RFU obtained from 10 randomly selected glomeruli; horizontal bars represent the mean RFU from the 3 mice in the respective age groups; the R^2 and p values for the correlation of RFU with age are shown and were derived from linear regression analysis). (**d**) Quantification of RFU shows changes in C3d deposition in glomeruli of MRL/lpr kidneys with disease progression (ages 8, 16 and 22 weeks; n = 3 mice per age group; RFU for each mouse is a mean RFU obtained from 10 randomly selected glomeruli; horizontal bars represent the mean RFU from the 3 mice in the respective age groups). Although C3d fragment is present in larger C3b/iC3b moieties, the anti-C3d antibody likely did not cross-react with these larger moieties. This is evident from the discrepancy in the pattern of staining (punctate for C3b/iC3b versus ribbon-like for C3d) and unparalleled changes in

intensity between C3b/iC3b and C3d on the MRL/lpr glomeruli from 16 to 22 weeks. Scale bar in (**b**) = 200 μm.

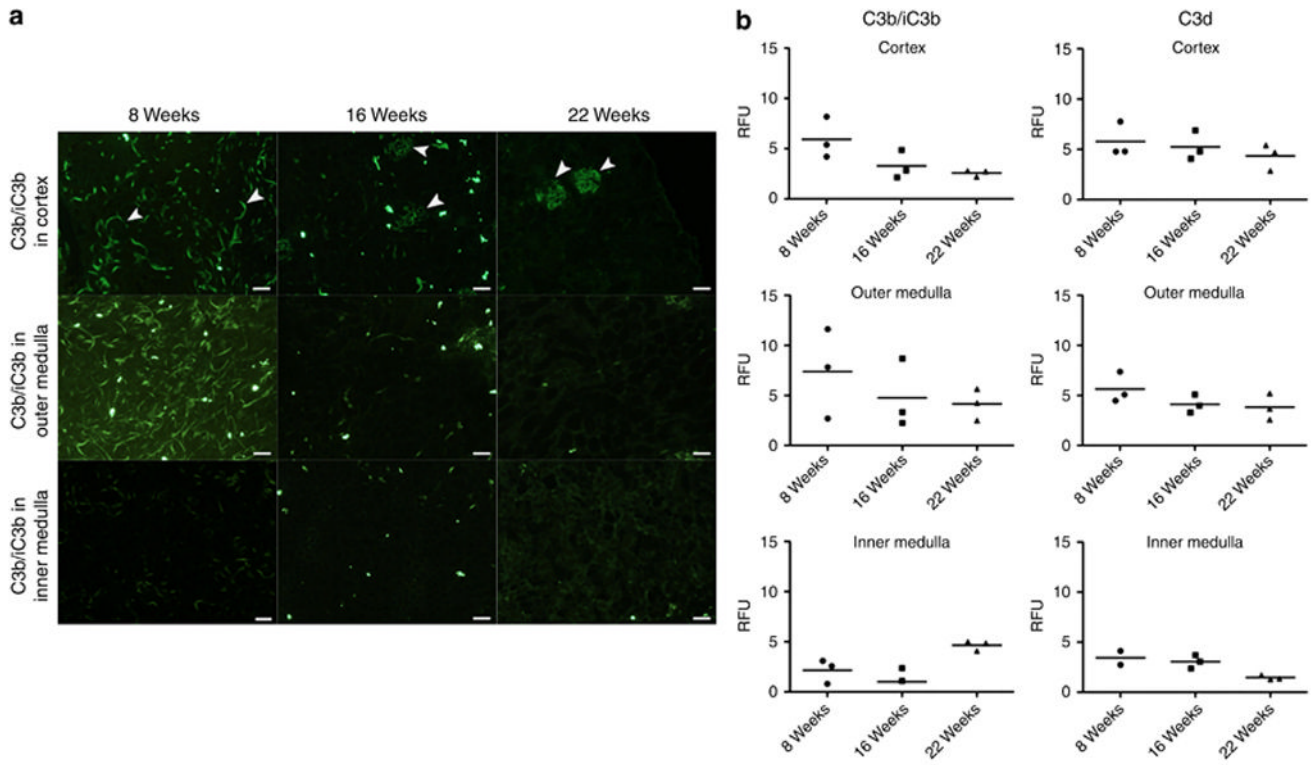

Figure 2. Tubular C3b/iC3b/C3d deposition in MRL/lpr mice reduces as the mice age

(**a**) Representative images of tubular staining for C3b/iC3b in cortex (top panel), outer medulla (middle panel) and inner medulla (bottom panel) of MRL/lpr kidneys are presented. Similar images were obtained for C3d immunostaining (images not shown). Arrowheads point to glomeruli. (**b**) Changes in tubular C3b/iC3b deposition in MRL/lpr mice as the mice age. Quantification of RFU shows a trend towards a decrease in tubular C3b/iC3b or C3d staining with disease progression (ages 8, 16 and 22 weeks; n = 2 mice for C3d staining inner medulla of 8 weeks old mice and n = 3 mice per age group for all other conditions; RFU for each mouse is a mean RFU obtained from 10 randomly selected tubules from each kidney compartment; horizontal bars represent the mean RFU from all the mice in the respective age groups). Scale bar in (**a**) = 200 μm.

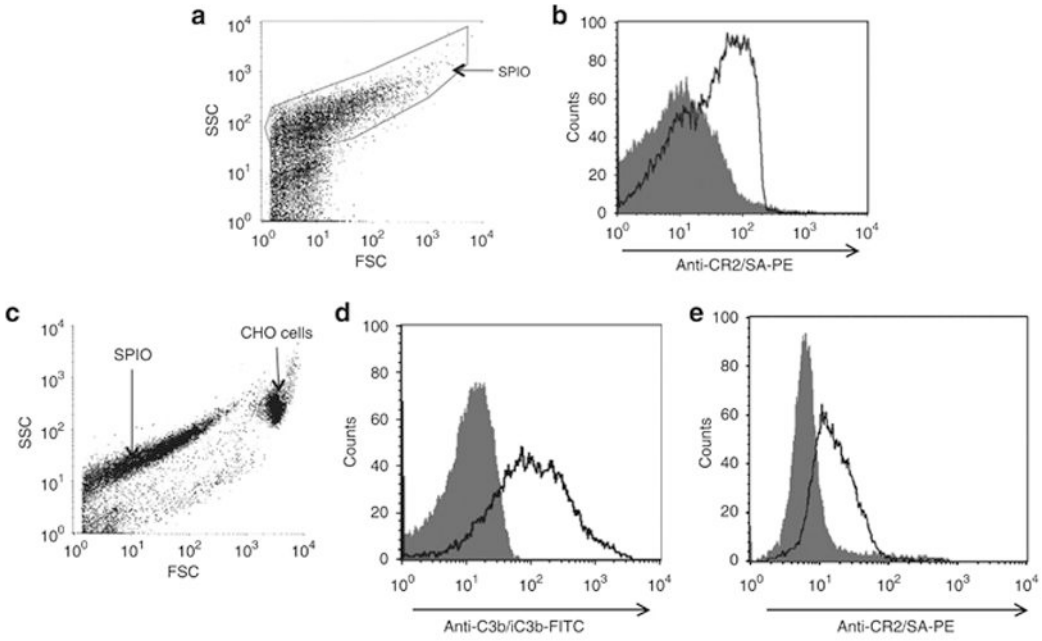

Figure 3. CR2-targeted SPIO bind to C3 fragments on opsonized CHO cells

(**a**) Dotplot diagram of CR2-targeted SPIO from flow cytometry analysis with forward scatter (FSC) on the horizontal axis and side scatter (SSC) on the vertical axis. (**b**) Flow cytometry profile of the gated SPIO in (**a**): histogram of untargeted SPIO (filled curve) is overlaid with histogram from CR2-targeted SPIO (black line). The horizontal axis represents the fluorescence intensity from biotinylated anti-CR2 antibody 171 and SA-PE (anti-CR2/SA-PE). The histogram shows that CR2-Fc was successfully conjugated to SPIO. (**c**) Dotplot diagram of opsonized CHO cells and CR2-targeted SPIO from flow cytometry analysis, same axes as in (**a**). (**d**) Histogram of unmanipulated CHO cells (filled curve) is overlaid with histogram from CHO cells opsonized with 10 percent mouse serum (black line). The deposition of C3b/iC3b on opsonized cells was confirmed with anti-C3b/iC3b-FITC labeled antibody. (**e**) Histogram of opsonized CHO cells incubated with CR2-targeted SPIO and unmanipulated 171 (filled curve) is overlaid with a histogram from opsonized CHO cells incubated with CR2-targeted SPIO and biotinylated 171. The horizontal axis represents the fluorescence intensity from anti-CR2/SA-PE.

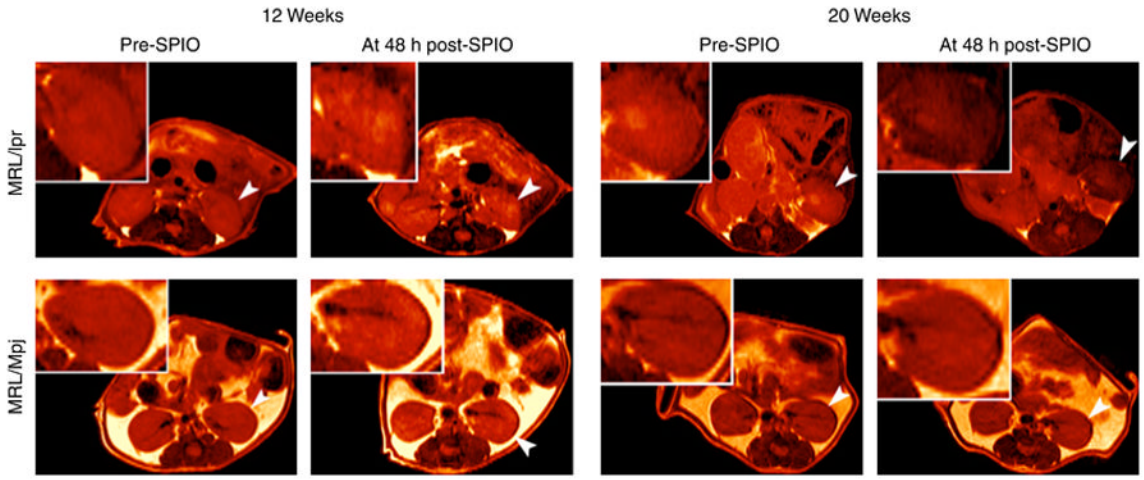

Figure 4. MR images of MRL/lpr and MRL/Mpj mice

Representative abdominal MR images at time to echo (TE) 20 ms of 12 and 20 weeks old MRL/lpr and MRL/Mpj mice taken prior to (pre-SPIO) and 48 h following (post-SPIO) CR2-targeted SPIO injection. The MR images are colored red for better visual presentation. A reduction in intensity is observed for left kidney (arrowhead and insert) from pre- to post-SPIO injection for 20 weeks old MRL/lpr mouse. In this same MRL/lpr mouse, the right kidney, although not as dark as the left, is darker than the right kidney of the same mouse at pre-SPIO injection. Of note, T2-relaxation times (determined from MR images of kidneys generated from 16 different TE) are a more sensitive measure for detecting SPIO-induced MRI signal reduction than visual evaluations of MR images, all of which are obtained at a single TE.

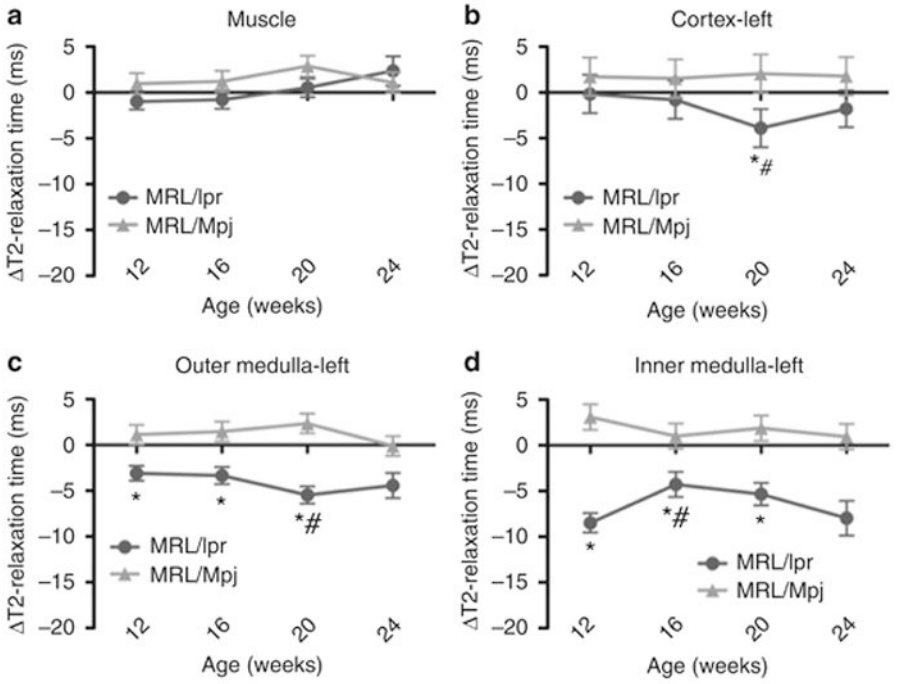

Figure 5. Non-invasive detection of glomerulonephritis progression

T2-relaxation times were measured prior to CR2-targeted SPIO injection and 48 h following injection. Changes in T2-relaxation times from pre-injected values (T2-relaxation times in milliseconds (ms)) for (**a**) muscle, (**b**) left kidney cortex, (**c**) outer medulla and (**d**) inner medulla of MRL/lpr and control MRL/Mpj mice at 12, 16, 20 and 24 weeks are presented. The right kidneys of MRL/lpr and MRL/Mpj mice had similar values (data not shown, Supplementary Table S1). When ΔT2-relaxation times were compared between the two strains, the MRL/lpr mouse kidneys show significantly reduced ΔT2-relaxation times at 20 weeks (cortex) and 12, 16 and 20 weeks (outer and inner medullae) from those of age- and area-matched MRL/Mpj mouse kidneys (* $p < 0.05$). When ΔT2-relaxation times were compared between the ages within the same strain, the MRL/lpr mouse kidneys showed a significant decrease in ΔT2-relaxation time at 20 weeks for cortex and outer medulla, and at 16 weeks for inner medulla (# $p < 0.05$) when compared to earlier ages.